Crystal Structure of the Complex of *Brugia malayi* Cyclophilin and Cyclosporin A[†,‡]

Paul J. Ellis,[§] Clotilde K. S. Carlow,[||] Dong Ma,[||] and Peter Kuhn*[,§]

Stanford Synchrotron Radiation Laboratory, SLAC, P.O. Box 4249, Bin 69, Stanford University, Stanford, California 94309, and New England Biolabs, 32 Tozer Road, Beverly, Massachusetts 01915

Received July 27, 1999; Revised Manuscript Received November 3, 1999

ABSTRACT: The resistance of the human parasite *Brugia malayi* to the antiparasitic activity of cyclosporin A (CsA) may arise from the presence of cyclophilins with relatively low affinity for the drug. The structure of the complex of *B. malayi* cyclophilin (BmCYP-1) and CsA, with eight independent copies in the asymmetric unit, has been determined at a resolution of 2.7 Å. The low affinity of BmCYP-1 for CsA arises from incomplete preorganization of the binding site so that the formation of a hydrogen bond between His132 of BmCYP-1 and *N*-methylleucine 9 of CsA is associated with a shift in the backbone of approximately 1 Å in this region.

The cyclophilins (CYPs)[1] are a family of proteins that bind the immunosuppressive drug cyclosporin A (CsA), a neutral 11-amino acid cyclic peptide originally isolated from the fungus *Tolypocladium inflatum*. CYPs have peptidyl−prolyl cis−trans isomerase (PPIase) activity, catalyzing the cis−trans isomerization of peptidyl−prolyl amide bonds, a slow step in protein folding (*1*). Because CsA contains a transition-state mimic of a peptidyl−prolyl bond undergoing isomerization, binding of CsA inhibits this activity (*2*). The immunosuppressive effect arises through the formation of a ternary complex of CYP−CsA with calcineurin, a protein serine phosphatase responsible for the dephosphorylation of important transcription factors (*3*). The T-cells of the immune system are particularly sensitive because they have relatively low levels of calcineurin (*3*).

Brugia malayi is a mosquito-transmitted filarial nematode parasite of humans in South and Southeast Asia. The worms reside in the lymphatic system, resulting in acute lymphangitis, "filarial fever", and lymphadenitis. Over the years, disturbances of the lymphatic system can lead to disfiguring elephantitis. It is estimated that more than 100 million people worldwide are infected by filarial parasites and more than 1 billion live in areas where filariasis is common (*4*).

Although CsA has been shown to possess potent antiparasite activity, *B. malayi* is not susceptible to this effect, possibly because of the presence of cyclophilins with low sensitivities to the drug (*5*, *6*). The 177-residue *N*-terminal cyclophilin-like domain of an unusual 843-residue two-domain protein from *B. malayi* has been cloned and overexpressed (*6*). Recombinant *B. malayi* cyclophilin (BmCYP-1) possesses PPIase activity with a sensitivity to CsA inhibition that is 40-fold reduced compared to that of human cyclophilin A (HuCYPA) (*6*). The crystal structure of uncomplexed BmCYP-1 has been determined (*7*, *8*).

We have determined the crystal structure of the complex of BmCYP-1 with CsA at a resolution of 2.7 Å. A comparison of this structure with uncomplexed BmCYP-1 and the complexed and uncomplexed forms of HuCYPA helps elucidate the structural basis of the low binding affinity.

EXPERIMENTAL PROCEDURES

Preparation of the Complex of BmCYP-1 with CsA. Primers were designed corresponding to the amino-terminal cyclophilin domain of BmCYP-1 (Genbank file L37292). The forward primer corresponded to the open-reading frame of BmCYP-1 and had the sequence 5′-ATGTCAAAAAAA-TCGCCGCCGGG-3′. The reverse primer (5′-CGGAAGCT-TCAAACAAGTTCACCACAATTAAGTAT-3′), corresponding to the 3′-end of the cyclophilin domain (including amino acid 177), contained a downstream termination codon and a *Hin*dIII recognition site (underlined). The primers were used in the following thermal cycling reaction: 10 pmol of each primer, 1× reaction buffer (NEB), each dNTP at 25 nM, and 100 ng of plasmid DNA and 1 unit of Vent DNA polymerase (NEB); cycled 20 times at 95 °C for 30 s, 55 °C for 30 s, and 72 °C for 30 s in 100 μL. The product was digested using *Hin*dIII and gel-purified from a 1.5% agarose

[†] This work is based upon research conducted at the Stanford Synchrotron Radiation Laboratory (SSRL). SSRL is funded by the Department of Energy (BES, BER) and the National Institutes of Health (NCRR, NIGMS). C.K.S.C. and D.M. thank Dr. D. Comb for financial support.

[‡] In accordance with journal and NIH policy, the coordinates of the structure discussed in this article have been deposited with the Protein Data Bank under file name 1C5F.

* Corresponding author. Telephone: (650) 926-3057. Fax: (650) 926-4100. E-mail: pkuhn@stanford.edu.

[§] Stanford University.

[||] New England Biolabs.

[1] Abbreviations: CYP, cyclophilin; CsA, cyclosporin A; PPIase, peptidyl−prolyl cis−trans isomerase; BmCYP-1, recombinant *B. malayi* cyclophilin; HuCYPA, human cyclophilin A; MoCYPC, mouse cyclophilin C; MeBmt, *N*-methyl-(4*R*)-4-[(*E*)-2-butenyl]-4-methyl-L-threonine; Abu, L-α-aminobutyric acid; Sar, *N*-methylglycine; MeLeu, *N*-methylleucine; MeVal, *N*-methylvaline; R_{merge}, $\Sigma_{hkl,i}|I_{hkl,i} - \langle I_{hkl}\rangle|/\Sigma_{hkl,i}\langle I_{hkl}\rangle$, where $I_{hkl,i}$ is a single measurement of an intensity and $\langle I_{hkl}\rangle$ is the merged intensity; F_o, observed structure factor; F_c, calculated structure factor; R, $\Sigma_{hkl}||F_o| - |F_c||/\Sigma_{hkl}|F_o|$, where F_o and F_c are the observed and calculated structure factors, respectively; rmsd, root-mean square deviation from ideality; R_{free}, free R factor.

10.1021/bi991730q CCC: $19.00
Published on Web 12/23/1999

gel using the Geneclean II Kit (BIO 101, Inc.). Following ligation into purified pMAL-c2 (NEB), which had been digested with *Xmn*I and *Hin*dIII, a fusion protein with maltose-binding protein (MBP) was generated. Plasmid DNA was isolated (Qiagen kit), and the insert was sequenced in both directions, establishing that no mutations had been generated during the PCR. Fusion protein was produced and purified as described in the MBP-fusion protein manual (NEB). Cleavage of MBP from the fusion protein was performed overnight at room temperature using a 0.1% factor Xa protease (NEB). Recombinant cyclophilin (177 amino acids) was separated from MBP by fast liquid chromatography (FPLC) using a Mono-Q anion exchange resin (Pharmacia). The homogeneous sample was then dialyzed overnight against 20 mM Tris (pH 8.0) and concentrated to 3 mg/mL in a Centricon 10 concentrator (Amicon).

The complex with CsA was prepared by mixing the BmCYP-1 solution with 5.0 mM CsA/methanol in a 1:1.7 molecular ratio and incubating overnight at 4 °C.

Crystallization and X-ray Data Collection. Crystals of the complex were grown using the hanging-drop vapor-diffusion method. The drop contained 2 μL of the complex solution, concentrated to 10 mg/mL BmCYP-1, and 2 μL of precipitating solution consisting of 20% (w/v) PEG 8000, 0.4 M calcium acetate, and 0.1 M MES (pH 6.0). The precipitating solution was also used in the reservoir. At 22 °C, clusters of colorless crystals, with the typical dimensions of individual crystals around 100 μm^3, grew in approximately 1 week.

A single crystal was placed in a cryoprotectant solution consisting of 16% PEG 8000, 20% (v/v) glycerol, 160 mM calcium acetate, and 80 mM MES (pH 6.0) for a few seconds. The crystal was then picked up with a fiber loop and flash-cooled in a stream of gaseous nitrogen at approximately 100 K. Diffraction data were collected from the frozen crystal using a MAR345 imaging plate detector on beam line 9-1 ($\lambda = 0.98$ Å) at the Stanford Synchrotron Radiation Laboratory. The data were processed using MOSFLM (*9*), and the programs SCALA and TRUNCATE from the CCP4 program package (*10*).

The crystal belongs to monoclinic space group $P2_1$ with the following cell dimensions: $a = 62.0$ Å, $b = 100.2$ Å, $c = 133.9$ Å, and $\beta = 93.8°$. A total of 409 247 measurements to 2.47 Å reduced to 56 200 unique reflections with a multiplicity of 2.9 and an R_{merge} of 0.120. As the diffraction was highly anisotropic, the data set is only 77.5% complete to 2.47 Å, using an $I/\sigma(I) = 1$ cutoff. To better indicate the quality of the data set, the reported resolution is that at which the 45 476 reflections with an $I/\sigma(I)$ of ≥ 1 would constitute a complete set. As calculated using the program XDL-DATAMAN (*11*) incorporated in the CCP4 package, 45 476 reflections are the same number as in a 100% complete data set to 2.68 Å.

Structure Determination. The structure was determined by the molecular replacement method using the known structure of BmCYP-1 taken from PDB entry 1A58 (*8*). The solution was obtained with the program AMoRE (*12*), incorporated in the CCP4 package, using data between 3 and 10 Å resolution and a search model obtained by removing all solvent molecules from the PDB entry. The 16 solutions from the cross-rotation function with the highest correlation coefficients (0.28−0.11) were used in a translation search. This generated 114 one-molecule solutions with correlation coefficients in the range of 0.22−0.15. For each of the these, a translation search for a second molecule was then conducted with each of the 16 rotations. To add subsequent molecules, the process was repeated for each of the 200 best unique solutions, but with an additional test that the packing arrangement was feasible. When no further molecules could be added, the best solution comprised eight molecules of BmCYP-1.

Table 1: Refinement Statistics

R	0.201
R_{free}	0.249
no. of reflections used	53355
no. of reflections omitted for R_{free}	2845
no. of protein atoms	11386
no. of water molecules	337
B_{av} (main chain)	43.1 Å^2
B_{av} (side chain)	43.8 Å^2
bond length rmsd	0.007 Å
bond angle rmsd	1.32°

To complete the starting model, the eight molecules of BmCYP-1 were refined using all data and the bound CsA molecules were added to correspond to density in a $F_o - F_c$ map.

Refinement and Validation of the Model. The structure was refined using alternating rounds of positional and temperature factor refinement with the program CNS (*13*), followed by manual rebuilding in annealed omit maps, also calculated with CNS, using the program XFIT from the XtalView package (*14*). Five percent of the data were randomly selected as the test set used to calculate R_{free} and were omitted from all refinements. A maximum-likelihood refinement target based on structure factors was used (*13*), permitting all remaining data to be included in the refinements.

Noncrystallographic symmetry restraints were applied in the initial stages of refinement, but were removed when it became apparent from the examination of annealed omit maps that the six N-terminal residues and many of the side chains did not have the same conformation in all eight BmCYP-1 molecules. A bulk solvent correction was used throughout, and, to compensate for the highly anisotropic diffraction, so was an overall anisotropic B factor (*15*).

In the final stage of refinement, solvent molecules, generated using the automated procedure in CNS in earlier stages, were removed. Solvent molecules were then added to the model in a stepwise fashion. For each step, (1) solvent molecules were added to correspond to the 50 highest peaks in an $F_o - F_c$ map with appropriate hydrogen-bonding contacts; (2) the model was refined to convergence; (3) an $F_o - F_c$ map was calculated, omitting the solvent, and any molecules corresponding to peaks of less than 3σ, with a real-space correlation coefficient of less than 0.8, or lying further than 3.5 Å from all potential hydrogen-bonding partners were deleted; and (4) the model was again refined to convergence. This process was repeated 37 times. After approximately 17 cycles, the number of water molecules removed in each cycle was close to the number added. The final solvent structure comprised the 337 molecules appearing in at least 18 of the final 20 models.

Refinement and stereochemical parameters for the final model are listed in Table 1. Representative omit map density for one of the eight bound CsA molecules is shown in Figure 1.

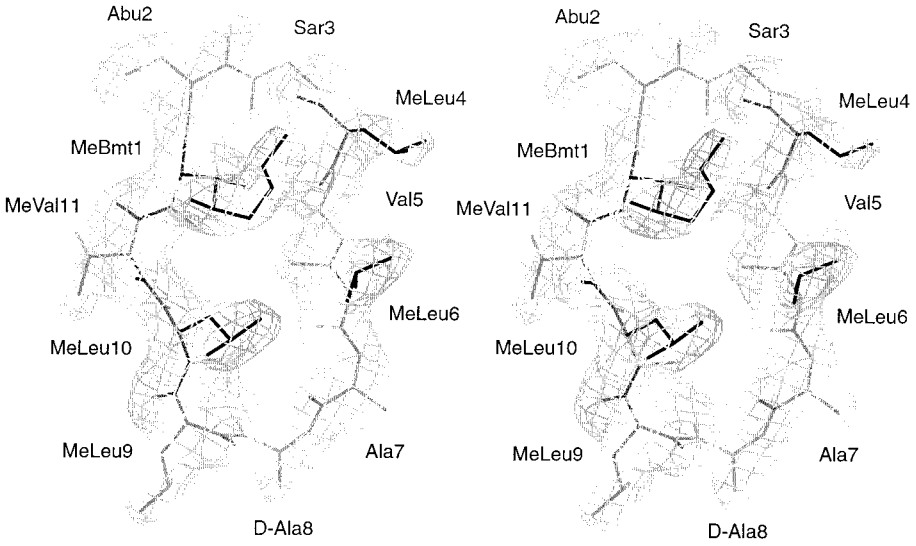

FIGURE 1: $F_o - F_c$ annealed omit map electron density for one of the eight independent bound CsA molecules, calculated using the final model and contoured at the 4σ level.

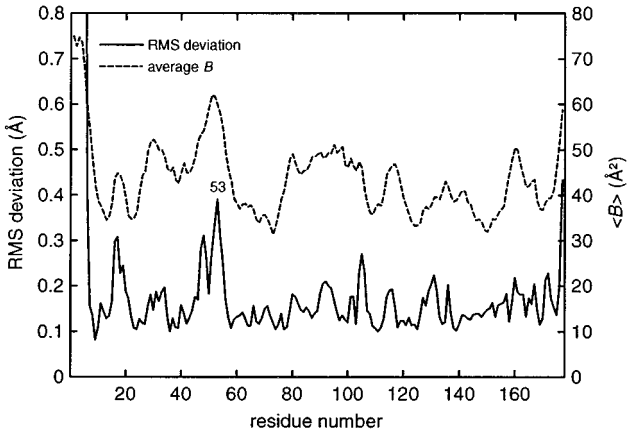

FIGURE 2: Plot of the rms deviation of the C, Cα, and N main chain atoms of the eight BmCYP-1 molecules from the average position (solid line). The average *B* factors for the atoms are also shown (dashed line).

The final model was analyzed using the program PROCHECK (*16*). All parameters are within acceptable limits. The Ramachandran plot shows 79.5% of protein residues in the most favored regions, 20.1% in the additional allowed regions, and the remaining 0.3% in the generously allowed regions.

To estimate the uncertainty in the model, the eight BmCYP-1 molecules were compared. Neglecting six residues at the N-terminus and one at the C-terminus, the rms deviation of the main chain (N, Cα, and C) atoms from the average is 0.17 Å and the maximum rms deviation is 0.39 Å at residue 53 (Figure 2). If we make the conservative assumption that the backbones are identical and that the deviation is due entirely to errors in the structure, an rms deviation from the average of 0.17 Å corresponds to an rms error in the individual atomic positions of 0.18 Å [$0.17 \times \sqrt{(8/7)}$] and an rms error in an averaged molecule of 0.06 Å ($0.18/\sqrt{8}$).

RESULTS AND DISCUSSION

The eight molecules of the BmCYP-1−CsA complex comprising the asymmetric unit are related by 2-fold and 2-fold screw noncrystallographic symmetry elements. Unlike the HuCYPA−CsA complex, which forms a decamer with 52 symmetry in the crystal (*18*), the eight molecules in the BmCYP-1−CsA crystal do not form any similar compact aggregate.

The overall structure of the BmCYP-1−CsA complex is an eight-stranded β-barrel capped by two α-helices (Figure 3), with the CsA molecule binding in a pocket formed by residues from the βD, DE, βE, EF, FG, βG, 3_{10}H, and HI segments.

Like the other CsA complexes for which crystal structures have been determined, HuCYPA−CsA (*17*, *18*) and mouse cyclophilin C−CsA (MoCYPC−CsA) (*19*), all amide bonds in the bound CsA molecule are in the trans conformation and there is one intramolecular hydrogen bond between the MeBmt1 side chain hydroxyl oxygen and the carbonyl oxygen of MeLeu4 [Oγ−O distance of 2.85 (0.12) Å, where the two figures are the average value and estimated standard deviation, respectively, calculated from the eight individual values].

As is generally the case in cyclophilins, the binding pocket is formed by 13 residues (Table 2) (*20*). The structure of the pocket is similar in all eight molecules of the complex. Figure 4 shows a superposition of the eight copies of the 13 residues in the pocket within 4.0 Å of the CsA molecule and the seven residues of CsA within 4.0 Å of the BmCYP-1 molecule. The only significant differences between the sites are in the conformation of the side chains of Lys114 and MeBmt1. When these atoms are neglected, the rms deviation of the eight sites from the average is just 0.18 Å.

The bound CsA molecule forms hydrogen bonds to Arg66, Gln74, Asn113, and His132 (Figure 5). The hydrogen-bonding pattern is similar to that seen in HuCYPA−CsA and MoCYPC−CsA, except that the interaction between the carbonyl O of MeBmt1 and Nϵ2 of Gln74 appears to be weak. Although the side chain of Gln74 has a similar conformation in all eight molecules, the program HBPLUS (*21*) classifies the contact as a hydrogen bond in only five of them and the average distance of 3.33 (0.22) Å is somewhat larger than that found in the CsA complexes of HuCYPA [3.10 (0.09) Å] and MoCYPC [3.11 (0.10) Å].

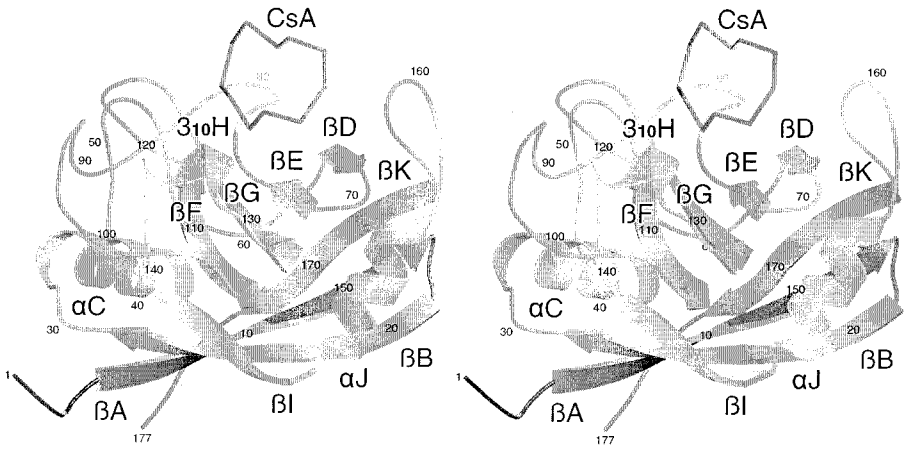

FIGURE 3: Stereo ribbon diagram of BmCYP-1 showing the cyclic CsA molecule in the binding site.

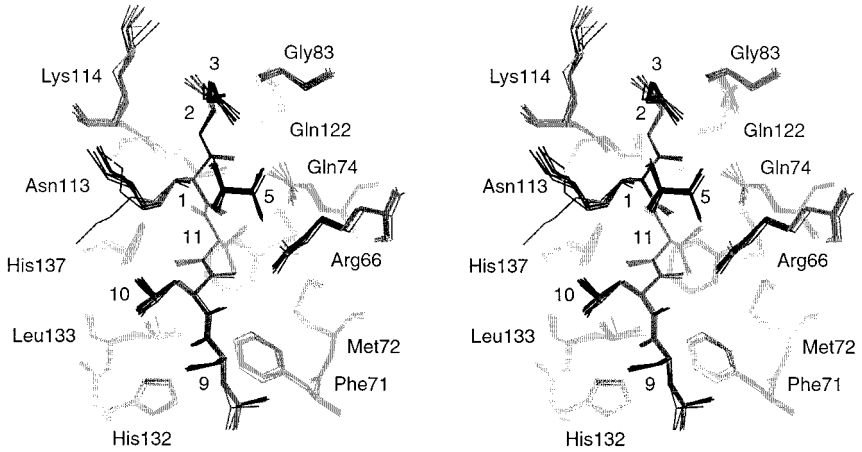

FIGURE 4: Superposition of the eight independent binding sites. All atoms of the 13 BmCYP-1 residues within 4.0 Å of the bound CsA molecule and the seven CsA residues within 4.0 Å of BmCYP-1 are shown. All BmCYP-1 residues except Ala112 and Phe124 are labeled. CsA residues MeBmt1, Abu2, Sar3, Val5, MeLeu9, MeLeu10, and MeVal11 are numbered.

Table 2: Interactions between CsA and BmCYP-1

CsA	BmCYP-1	distance (Å)
	Hydrogen Bonds	
MeBmt1 O	Gln74 Nϵ2	3.33 (0.22)
Abu2 N	Asn113 O	2.84 (0.13)
MeLeu9 O	His132 Nϵ2	2.76 (0.13)
MeLeu10 O	Arg66 Nη1	2.95 (0.21)
	Arg66 Nη2	2.86 (0.21)
	Hydrophobic or Polar Interactions[a,b]	
MeBmt1	Arg66, Gln74, Asn113, Lys114, His137	
Abu2	Gly83, Ala112, Asn113, Lys114, Gln122	
Sar3	Gly83	
Val5	Arg66	
MeLeu9	Phe71, His132, Leu133	
MeLeu10	Arg66, Phe71	
MeVal11	Arg66, Phe71, Met72, Gln74, Ala112, Asn113, Phe124, Leu133, His137	

[a] A distance of less than 4.0 Å is defined as a hydrophic or polar interaction. [b] Interactions appearing in only one of the eight molecules were neglected.

Comparison with Uncomplexed BmCYP-1. There are substantial changes in the structure of BmCYP-1 associated with CsA binding, the largest of which are localized to the binding site. Figure 6 shows the mean deviation of the main chain atoms of complexed BmCYP-1 from uncomplexed BmCYP-1, together with a comparison to the corresponding differences between the individual molecules in the complexed state. If the first of the three highest peaks is considered, it is clear that the magnitudes of the differences between the complexed and uncomplexed states in the vicinity of Gly54 are comparable to those between unique molecules in the same state and that the size of the peak is substantially reduced by subtracting the curves. The deviations in this region were ascribed principally to the effect of extraneous influences, such as packing forces, on a conformationally free surface loop, and are not considered significant. After a similar analysis of the remaining peaks, the third, at the binding site residue His132, is approximately twice as high as the second, at Asp104.

Figure 7 shows a comparison of the pocket in the complexed and uncomplexed states. As predicted by Mikol et al. (*7*) and Taylor et al. (*8*), the most significant differences are as follows: (1) the side chain of Lys114, which, in the uncomplexed state, is stabilized by a hydrogen bond to the carbonyl oxygen of Gly83 (Nζ−O distance of 2.8 Å) in a position obstructing the CsA residue Abu2, is rotated into the solvent, with the loss of the hydrogen bond; (2) His132 moves approximately 1 Å toward the CsA molecule to form a hydrogen bond to the carbonyl oxygen of MeLeu9 [Nϵ2−O distance of 2.76 (0.13) Å]; (3) Phe71 is rotated approximately 25°, moving the center of the phenyl ring 2 Å in a direction similar to that of the His132 displacement; and (4) the side chain of Arg66 changes conformation to form two hydrogen bonds to the carbonyl oxygen of MeLeu10. The motion of Phe71 appears to be due to contacts

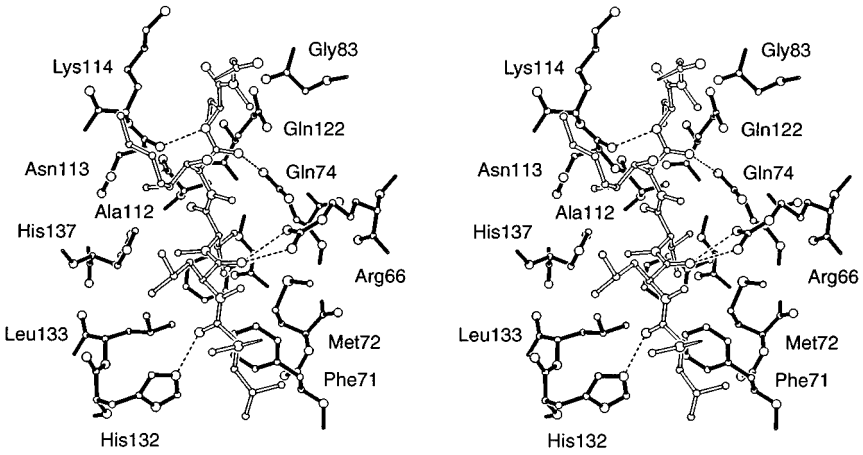

FIGURE 5: Stereoview of the BmCYP-1 binding site of molecule A, showing the 13 residues from BmCYP-1 (solid bonds) and six of the seven residues from CsA (hollow bonds) involved in the interaction. The Val5 residue of CsA, the side chain of which lies within 4.0 Å of the side chain of Arg66 in seven of the eight complexes, has been omitted for clarity. All BmCYP-1 residues except Phe124 are labeled. The five hydrogen bonds between BmCYP-1 and CsA are shown as dashed lines.

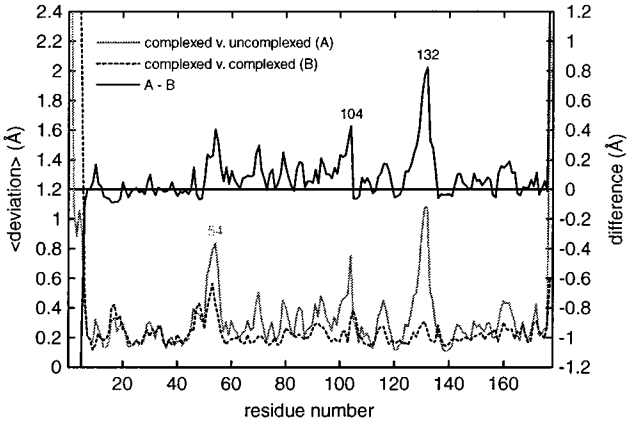

FIGURE 6: Plot of the mean deviation of the C, Cα, and N main chain atoms of the eight complexed BmCYP-1 molecules from the uncomplexed form, taken from PDB entry 1A58 (gray line). Also shown are the mean deviations between the complexed molecules (dashed line) and the difference between the two curves (solid black line).

with the side chain of Ala130, which moves approximately 1 Å with His132 toward Phe71 on CsA binding, rather than any direct interaction with CsA, as the side chain in the uncomplexed orientation lies approximately 4.0 Å from the CsA molecule, but has short contacts with the bound positions of Ala130 (Cζ−Cβ distance of ≈2.7 Å). Other differences include a slight change in the conformation of the side chain of Met72.

Comparison with HuCYPA. Human cyclophilin A from T-cells is the best characterized of the cyclophilin family, with more than 30 crystal structures of HuCYPA and complexes of HuCYPA with CsA, CsA analogues, and oligopeptide substrates currently available, compared to two for BmCYP-1, the next most well represented. The sensitivity of HuCYPA to inhibition by CsA (IC_{50} = 19 nM) is 40 times higher than that of BmCYP-1 (IC_{50} = 860 nM) (*6*). This difference arises because, whereas the binding site in BmCYP-1 requires substantial changes to accommodate CsA, the binding pocket in HuCYPA does not (Figure 8).

Although the degree of sequence identity between BmCYP-1 and HuCYPA is only 49%, the binding site is highly conserved. Of the 13 residues, only two are not identical: Lys114 and His132 in BmCYP-1 corresponding to Ala103 and Trp121 in HuCYPA (*6*).

Site-directed mutagenesis of Lys114 and His132 has shown that of the two differences compared to HuCYPA, the presence of histidine rather than tryptophan at position

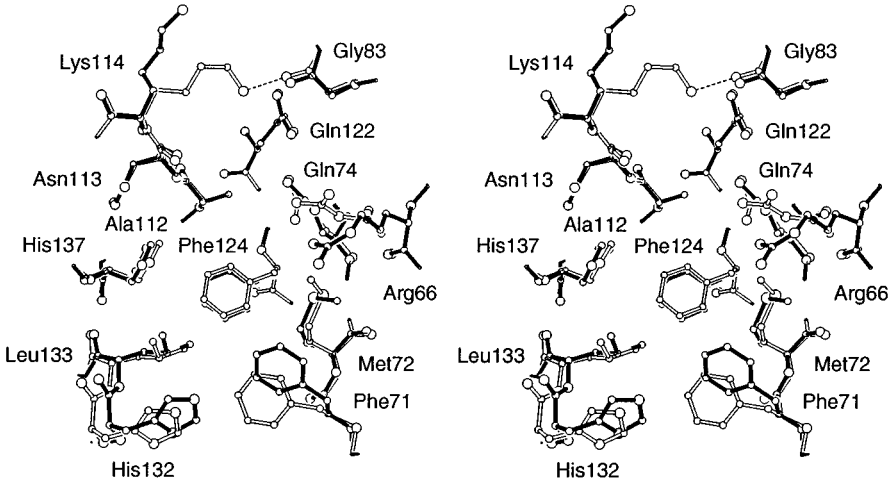

FIGURE 7: Stereoview of the BmCYP-1 binding site, showing the differences between the complexed state (solid bonds) and the uncomplexed state (hollow bonds). The hydrogen bond stabilizing the position of the side chain of Lys114 in the uncomplexed state is shown as a dashed line.

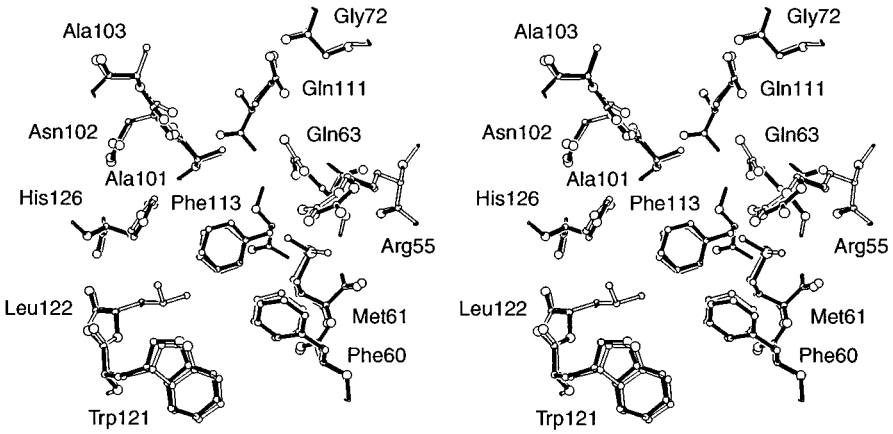

FIGURE 8: Stereoview of the HuCYPA binding site, showing the differences between the complexed state (solid bonds) and the uncomplexed state (hollow bonds).

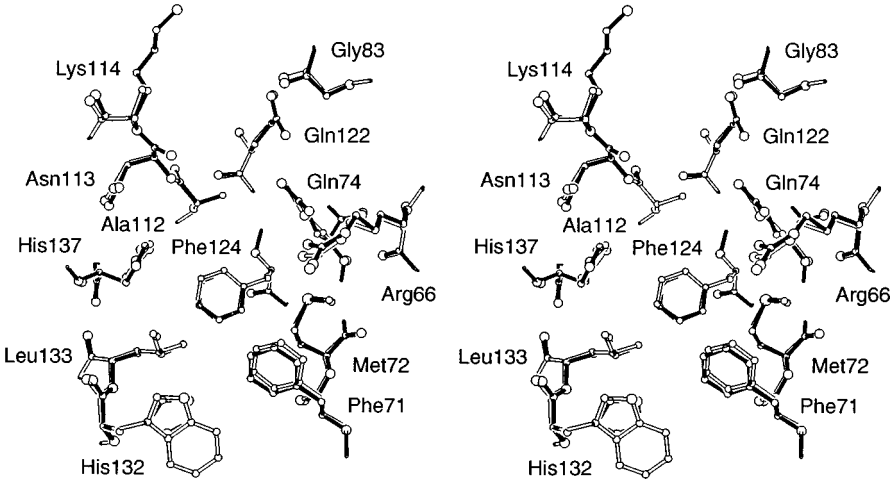

FIGURE 9: Stereoview of the BmCYP-1 binding site in the complexed state (solid bonds) superposed on the HuCYPA binding site in the complexed state (hollow bonds).

132 is the primary determinant of the lower CsA affinity (*20*). Replacement of His132 with tryptophan enhanced the susceptibility of BmCYP-1 to CsA inhibition by a factor of 9. In contrast, replacement of Lys114 by alanine reduced the extent of inhibition by a factor of 2. Mutation of both residues increased the extent of inhibition by a factor of 17.

Although binding of CsA requires that the hydrogen bond between the side chain of Lys114 and the carbonyl of Gly83 be broken, this rearrangement of a single side chain does not have a strong effect on CsA binding. In contrast, the structural changes in the vicinity of His132 are much more extensive and include backbone displacements of approximately 1 Å as well as the displacement of the side chain of Phe71 by approximately 2 Å (Figure 7).

Likewise, although the conformation of the side chain of Arg66 in uncomplexed BmCYP-1 also differs from that of Arg55 in HuCYPA, this is not considered significant since (1) the backbone atoms of the residue have closely similar positions in BmCYP-1 and HuCYPA, in both the complexed and uncomplexed states; (2) the side chains, which form hydrogen bonds to the carbonyl oxygen of MeLeu10, adopt closely similar conformations in the complex; (3) the only residue with which it forms intramolecular hydrogen bonds, Gln74 in BmCYP-1 and Gln63 in HuCYPA, is also closely similar in BmCYP-1 and HuCYPA in both states; and (4) the conformation of the side chain in uncomplexed BmCYP-1 is strongly influenced by contacts with a neighboring molecule (*7*).

Finally, we note the similarity of the binding site in the BmCYP-1−CsA complex and that in the HuCYPA−CsA complex. In the complexed state, the five-membered ring of His132 corresponds closely to the five-membered ring of Trp121 as do the phenyl rings of Phe71 and Phe60 (Figure 9). When the corresponding atoms of the five-membered rings are considered as equivalent, and the atoms beyond Cβ in Lys114 are neglected, the rms difference for all atoms in the site is just 0.32 Å, compared to 1.0 Å in the uncomplexed state.

CONCLUSION

The new structure of the complex of BmCYP-1 is consistent with the suggestion by Mikol et al. (*7*) and Taylor et al. (*8*) that the reduced affinity of BmCYP-1 for CsA compared to that of HuCYPA arises from incomplete preorganization of the binding site in the vicinity of His132 so that the formation of a hydrogen bond between the Nϵ2 atom of His132 and the carbonyl oxygen of the MeLeu9 residue of CsA is associated with a shift in the backbone of approximately 1 Å in this region and the displacement of the side chain of Phe71 by approximately 2 Å. One of the five hydrogen bonds between BmCYP-1 and CsA also

appears to be weaker than the corresponding bond in the complex of CsA with HuCYPA or MoCYPC.

ACKNOWLEDGMENT

C.K.S.C. and D.M. thank Dr. I. Schildkraut for advice and encouragement.

REFERENCES

1. Fischer, G., Wittmann-Liebold, B., Lang, K., Kiefhaber, T., and Schmidt, F. (1989) *Nature 337*, 473.
2. Schreiber, S. L. (1991) *Science 251*, 283−287.
3. Schreiber, S. L., and Crabtree, G. R. (1992) *Immunol. Today 13*, 136−142.
4. World Health Organization (1991) Tropical Diseases Progress in Research Report, Geneva, Switzerland.
5. Page, A. P., Kumar, S., and Carlow, C. K. S. (1995) *Parasitol. Today 11*, 385−388.
6. Page, A. P., Landry, D., Wilson, G. G., and Carlow, C. K. S. (1995) *Biochemistry 34*, 11545−11550.
7. Mikol, V., Ma, D., and Carlow, C. K. S. (1998) *Protein Sci. 5*, 1310−1316.
8. Taylor, P., Page, A. P., Kontopidis, G., Husi, H., and Walkinshaw, M. D. (1998) *FEBS Lett. 425*, 361−366.
9. Leslie, A. G. W. (1992) in *Joint CCP4 and ESF-EACBM Newletter on Protein Crystallography, No. 26*, SERC Daresbury Laboratory, Warrington, U.K.
10. Collaborative Computational Project Number 4 (1994) *Acta Crystallogr. D50*, 760−763.
11. Kleywegt, G. J., and Jones, T. A. (1996) *Acta Crystallogr. D52*, 826−828.
12. Navaza, J. (1994) *Acta Crystallogr. A50*, 157−163.
13. Brünger, A. T., Adams, P. D., Clore, G. M., DeLano, W. L., Gros, P., Grosse-Kunstleve, R. W., Jiang, J.-S., Kuszewski, J., Nilges, M., Pannu, N. S., Read, R. J., Rice, L. M., Simonson, T., and Warren, G. L. (1998) *Acta Crystallogr. D54*, 905−921.
14. McRee, D. E. (1993) *Practical Protein Crystallography*, Academic Press, San Diego, CA.
15. Jiang, J.-S., and Brünger, A. T. (1994) *J. Mol. Biol. 243*, 100−115.
16. Laskowski, R. A., MacArthur, M. W., Moss, D. S., and Thornton, J. M. (1993) *J. Appl. Crystallogr. 26*, 283−291.
17. Mikol, V., Kallen, J., Pfluegl, G., and Walkinshaw, M. D. (1993) *J. Mol. Biol. 234*, 1119−1130.
18. Ke, H., Mayrose, D., Belshaw, P. J., Alberg, D. G., Shreiber, S. L., Chang, Z. Y., Etzkorn, F. A., Ho, S., and Walsh, C. T. (1994) *Structure 2*, 33−44.
19. Ke, H., Zhao, Y., Luo, P., Weissman, I., and Friedman, J. (1993) *Proc. Natl. Acad. Sci. U.S.A. 90*, 11850−11854.
20. Ma, D., and Carlow, C. K. S. (1998) *Mol. Biochem. Parasitol. 92*, 361−365.
21. McDonald, I. K., and Thornton, J. M. (1994) *J. Mol. Biol. 238*, 777−793.

BI991730Q